

Work Records for the Event Generator of Quasielastic ${}^2H(\vec{e}, e' \vec{n}){}^1H$

Tongtong Cao
Hampton University

March 26, 2018

Chapter 1

Record 1

1.1 About Generator

There are four parallel channels in the generator. For each channel, there are 3 parallel filters to select events. To produce a file, a fixed channel with a fixed filter is chosen.

The axis coordinates are defined in the lab frame. z is along the electron beam, y is perpendicular to the hall floor, and x is y cross z.

1.2 Initial Setup

When running the generator, some parameters are initially set, including beam energy (E), beam polarization (P_e), ratio of events with positive helicity to with negative helicity, polar angle of neutron polarimeter (θ_n), open angle of the detectors for scattered electrons, neutron electric form factor (G_E^n) and neutron magnetic form factor (G_M^n).

After E and θ_n are given, all kinematics can be calculated assuming the target is free neutron and the electron mass is 0, including Q^2 , energy of scattered electron (E'), polar angle of scattered electron (θ_e) and momentum of recoiled neutron (p_n). Formulas are

$$p_n = 2m_n E(m_n + E) \cos \theta_n / (2m_n E + m_n^2 + E^2 \sin^2 \theta_n), \quad (1.1)$$

$$E' = \sqrt{(p_n \sin \theta_n)^2 + (E - p_n \cos \theta_n)^2}, \quad (1.2)$$

$$Q^2 = 2m_n(E - E'), \quad (1.3)$$

$$\theta_e = 2 \sin^{-1}(\sqrt{m_n(E - E')/(2EE')}). \quad (1.4)$$

If G_E^n is not assigned, it is calculated by

$$G_E^n = -a\mu_n\tau G_D/(1 + b\tau) \quad (1.5)$$

where $\tau = Q^2/4m_n^2$, $G_D = (1 + Q^2/\Lambda^2)^{-2}$, $\Lambda^2 = 0.71 \text{ (GeV}/c)^2$, $a = 0.886$, and $b = 3.29$. The formula from the CGEN proposal is obtained by fitting experimental data to the Galster parameterization.

If G_M^n is not assigned, it is calculated by

$$G_M^n = \frac{\mu_n}{1 + \frac{Q^2 b_1}{1 + \frac{Q^2 b_2}{1 + \frac{Q^2 b_3}{1 + \frac{Q^2 b_4}{1 + Q^2 b_5}}}}} \quad (1.6)$$

where $b_1, \dots, b_5 = 3.26, 0.272, 0.0123, -2.52, 2.55 \text{ (GeV}/c)^{-2}$. The formula refers to G. Kubon (2002).

1.3 channels

1.3.1 Channel 1

Channel 1 is for the reaction $\vec{e}n \rightarrow e\vec{n}$ where the target is free neutron. Firstly, The phase space calculation is implemented, then events with scattered electrons located in the detector open angle are kept, and finally a filter is used to select events. There are three types of filters: 1) no filter 2) unpolarized Differential Cross Section (DCS) 3) polarized DCS.

Unpolarized DCS is expressed as

$$\sigma_0 = \sigma_{Mott} \frac{E'}{E} \frac{1}{\epsilon(1+\tau)} [\tau(G_M^n)^2 + \epsilon(G_E^n)^2] \quad (1.7)$$

where $\sigma_{Mott} = \frac{\alpha^2 \cos^2(\theta_e/2)}{4E^2 \sin^4(\theta_e/2)}$, α is the fine structure const, and $\epsilon = [1 + 2(1+\tau) \tan^2(\theta_e/2)]^{-1}$.

Polarized DCS is expressed as

$$\sigma = \sigma_0(P^{(0)} + hP^{(h)}) \quad (1.8)$$

where $P^{(0)}$ denotes the helicity-independent recoil polarization, $P^{(h)}$ denotes the helicity-dependent recoil polarization and $h = \pm 1$ denotes the electron helicity. The polarization is customarily projected onto a $(\hat{t}, \hat{n}, \hat{l})$ unit vector basis, with the longitudinal component, \hat{l} , along the recoil nucleon's momentum; the normal component, \hat{n} , perpendicular to the electron scattering plane; and the transverse component, \hat{t} , perpendicular to the \hat{l} component in the scattering plane. In the one-photon exchange approximation, $P^{(0)} = 0$, and $P^{(h)}$ is confined to the scattering plane (i.e., $P_n^{(h)} = 0$). The transverse, $P_t^{(h)}$, and longitudinal, $P_l^{(h)}$, components are expressed in terms of kinematics and nucleon form factors as

$$P_t^{(h)} = P_e \frac{-2G_E^n G_M^n \sqrt{\tau(1+\tau)} \tan(\theta_e/2)}{(G_E^n)^2 + [\tau + 2\tau(1+\tau) \tan^2(\theta_e/2)](G_M^n)^2}, \quad (1.9)$$

$$P_l^{(h)} = P_e \frac{2(G_M^n)^2 \tau \sqrt{(1+\tau)(1+\tau \sin^2(\theta_e/2))} \sec(\theta_e/2) \tan(\theta_e/2)}{(G_E^n)^2 + [\tau + 2\tau(1+\tau) \tan^2(\theta_e/2)](G_M^n)^2} \quad (1.10)$$

The phase-shift is defined as

$$\delta = \frac{P_t^{(h)}}{P_l^{(h)}} = -\frac{G_E^n}{G_M^n} \frac{\cos(\theta_e/2)}{\sqrt{\tau + \tau^2 \sin^2(\theta_e/2)}}. \quad (1.11)$$

The formulas refer to B. Plaster (2006) and Raymond G. Arnold (1980). Note: the expression of formula (2b) in B. Plaster (2006) is not correct, and the expressions of formulas 7 and 8 in PAC45 for PR12-17-004 are not correct.

1.3.2 Channel 2

Channel 2 is for the quasielastic reaction $\vec{e}d(np) \rightarrow e\vec{n}(p)$ where electron reacts with neutron bound in deuteron and proton is a spectator. Firstly, Fermi momentum is randomly generated by the Paris model and Lorentz vectors of neutron and proton are built where neutron is on-shell and proton is off-shell, then electron reacts with momentumized neutron, next the phase space calculation is implemented and events with scattered electrons located in the detector open angle are kept, and finally a filter is used to select events. There are three types of filters: 1) no filter 2) unpolarized DCS 3) polarized DCS.

Approximately, the formulas of unpolarized and polarized DCS in channel 1 are applied into this channel. But for events with the same beam energy, calculated values of unpolarized DCS, $P_t^{(h)}$ and $P_l^{(h)}$ are different between the two channels since kinematics are different. Additionally, the definition of \hat{t} , \hat{n} , \hat{l} in channel 1 is not applicable for this channel since recoiled neutron may not be in the electron scattering plane. In fact, the recoil polarization can not be simply expressed as the definition in channel 1 when the target neutron has momentum.

1.3.3 Channel 3

Kinematics of channel 3 are the same as channel 2. But unpolarized DCS is theoretically calculated as

$$\sigma_0 = \frac{1}{4} \frac{E'^2}{m_n^2 E^2} |M|^2, \quad (1.12)$$

$$|M|^2 = \frac{4\alpha^2}{Q^4} \{K_1(\tilde{P}_e \cdot \tilde{P}_{e'}) + K_2[\frac{(\tilde{P}_e \cdot \tilde{P}_n)(\tilde{P}_{e'} \cdot \tilde{P}_n)}{m_n^2} - \frac{Q^2}{4}]\} \quad (1.13)$$

where M is amplitude, $K_1 = Q^2(G_M^n)^2$, $K_2 = 4m_n^2 \frac{(G_E^n)^2 + \tau(G_M^n)^2}{1+\tau}$, \tilde{P}_e is Lorentz vector of incoming electron, $\tilde{P}_{e'}$ is Lorentz vector of scattered electron, and \tilde{P}_n is Lorentz vector of target neutron with Fermi momentum. The calculation refers to Griffiths's book "Introduction to Elementary Particles".

Study of polarized DCS for $\vec{e}n \rightarrow e\vec{n}$ where the target neutron has Fermi momentum is underway. Currently, the formula of polarized DCS in channel 1 is applied. The unpolarized DCS defined here is substituted into the formula.

1.3.4 Channel 4

Channel 4 is for the electrodisintegration of deuteron $\vec{e}d \rightarrow e\vec{n}p$. The phase space calculation is implemented and events with scattered electrons located in the detector open angle are kept.

Currently, no filters are applied to select events. Study of DCS and recoil polarization for this channel is underway.

1.4 Programming

1.4.1 Support Tools

The program is made with support of C++ and ROOT, and the build tool is Make.

1.4.2 Source files

All source files in the package list as

- Makefile: script for compilation
- edQuasiElastic.cc: main function
- JGenFermiMomentum.h and JGenFermiMomentum.cc: a class to generate Fermi momentum of nucleons bound in deuteron using the Paris model
- JGenPhaseSpace.h and JGenPhaseSpace.cc: a class to implement phase space calculation for reactions with 2 or 3 or 4 products.

1.4.3 Options

Some options are provided to run the program.

- h Show options
- R [filename] ROOT output to filename
- M [#] Generate number (#) of events; default: 1
- C [channel] Channel is processed; one of four parallel channels is chosen; Default: 3
- F [filter] Choose a filter to select events
 - filter='n' no filter
 - filter='u' unpolarized DCS
 - filter='p' (default) polarized DCS
- E [energy] Electron beam energy (GeV); default: 2.2

-H [ratio]	Ratio of events with helicity + to with helicity - for electron beam; default: 1
-P [polarization]	Polarization of electron beam; default: 0.8
-O [openAngle]	Open angle of the detector for scattered electrons (deg); default: 5
-T [angle]	Polar angle of neutron polarimeter (deg); default: 28
-e [GEn]	Neutron electronic form factor; if not assigned, G_E^n is calculated by formula
-m [GMn]	Neutron magnetic form factor; if not assigned, G_M^n is calculated by formula

1.4.4 How to Run

After compilation, the executable file “edQuasiElastic” is produced. Here is an example to run the program.

```
./edQuasiElastic -R test.root -C 3 -F u -M 10000
```

where the name of output root file is test.root, channel 3 with the unpolarized DCS filter is chosen, and 10000 events are generated. Defaults are used for other options.

1.4.5 Branches of Output Root File

Branches of output root file list as

- event: event number
- x, y, z: location of vertex; useless currently
- q2, energySElectron, thetaSElectron, pRNeutron, thetaRNeutron, tau, epsilon: Q^2 , E' , θ_e , p_n , θ_n , τ , ϵ
- unpolDCS, polDCS, polTrans, polLongi, helicity: unpolarized DCS, polarized DCS, $P_t^{(h)}$, $P_l^{(h)}$, helicity
- beam, target, spectator, w, p1, p2, p3: Lorentz vectors of beam, target neutron and spectator proton with Fermi momentum specified for channel 2 and 3, beam+target, the first product (electron), the second product (neutron), the third product (proton) specified for channel 4

1.5 Production and Analysis

1.5.1 Production

10 files are produced. The beam energy is 2.2 GeV for all files. Files 1-3 are for channel 1 with no, unpolarized DCS and polarized DCS filters respectively, files 4-6 are for channel 2 with no, unpolarized DCS and polarized DCS filters respectively, files 7-9 are for channel 3 with no, unpolarized DCS and polarized DCS filters respectively, and file 10 is for channel 4 with no filter. Other initial parameters are default values, and G_E^n and G_M^n are calculated by the formulas. The initial setup lists as $E = 2.2$ GeV, $\theta_e = 28$ deg, $openangle = 5$ deg, $G_E^n = 0.0207221$, and $G_M^n = -0.122691$, then other kinematics are calculated as $Q^2 = 2.19011$ (GeV/c)², $E' = 1.03451$ GeV, $\theta_e = 58.7449$ deg, and $p_n = 1.88374$ GeV/c.

1. ./edQuasiElastic -M 100000 -C 1 -F n -R c1n.root
2. ./edQuasiElastic -M 100000 -C 1 -F u -R c1u.root
3. ./edQuasiElastic -M 100000 -C 1 -F p -R c1p.root
4. ./edQuasiElastic -M 100000 -C 2 -F n -R c2n.root
5. ./edQuasiElastic -M 100000 -C 2 -F u -R c2u.root
6. ./edQuasiElastic -M 100000 -C 2 -F p -R c2p.root
7. ./edQuasiElastic -M 100000 -C 3 -F n -R c3n.root

8. ./edQuasiElastic -M 100000 -C 3 -F u -R c3u.root
9. ./edQuasiElastic -M 100000 -C 3 -F p -R c3p.root
10. ./edQuasiElastic -M 100000 -C 4 -F n -R c4n.root

1.5.2 Analysis

Figure 1.1 shows Fermi momentum of neutron (left) and proton (right) bound in deuteron.

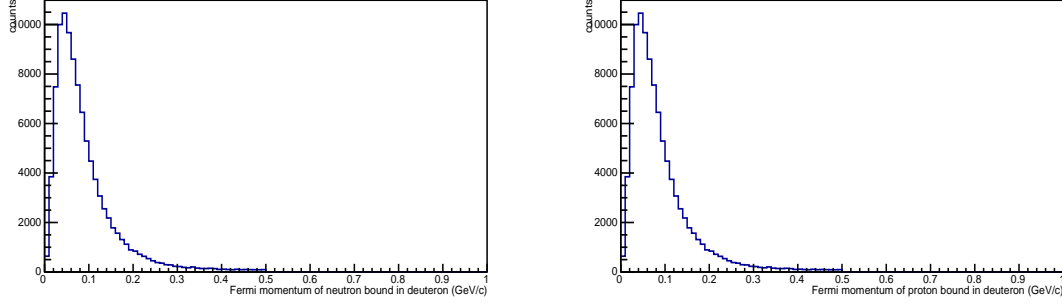


Figure 1.1: Fermi momentum

Figure 1.2 shows comparisons of kinematics between 4 channels without filter. Kinematics includes Q^2 (top left), E' (top right), θ_e (middle left), P_n (middle right), and θ_n (bottom left). The red line denotes channel 1, the green line denotes channel 2, the blue line denotes channel 3, and the black line denotes channel 4. The difference between channel 1 and channel 2&3 is caused by Fermi momentum. Channel 4 is for electron disintegration of deuteron including all of nuclear effects.

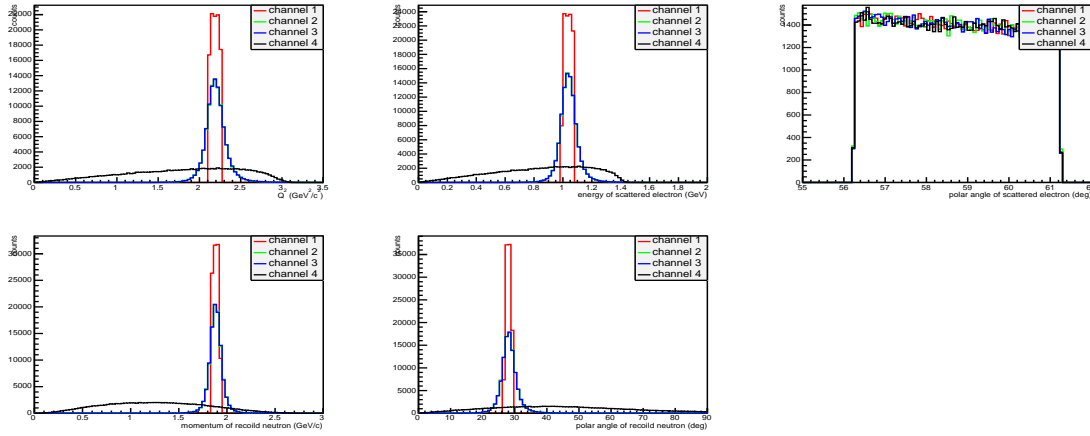


Figure 1.2: Comparisons of Kinematics between 4 channels without filter

Figure 1.3 shows kinematics for channel 4 without filter with momentum of produced proton less than 0.2 GeV/c. After cut, events are mainly from quasielastic, so the distributions become close to channels 2&3.

Figure 1.4 shows DCS information, such as unpolarized DCS (left), $P_t^{(h)}$ (middle) and $P_l^{(h)}$ (right). The same unpolarized DCS formula is applied for channels 1 and 2, but kinematics of them are not the same. For channels 2 and 3, kinematics of them are the same, but the unpolarized DCS formula is not the same. Currently, the same $P_t^{(h)}$ (middle) and $P_l^{(h)}$ formulas are applied into channels 1, 2 and 3.

Figure 1.5 shows comparisons of kinematics between filters for channel 3. Kinematics includes Q^2 (top left), E' (top right), θ_e (middle left), P_n (middle right), and θ_n (bottom left). The red line denotes

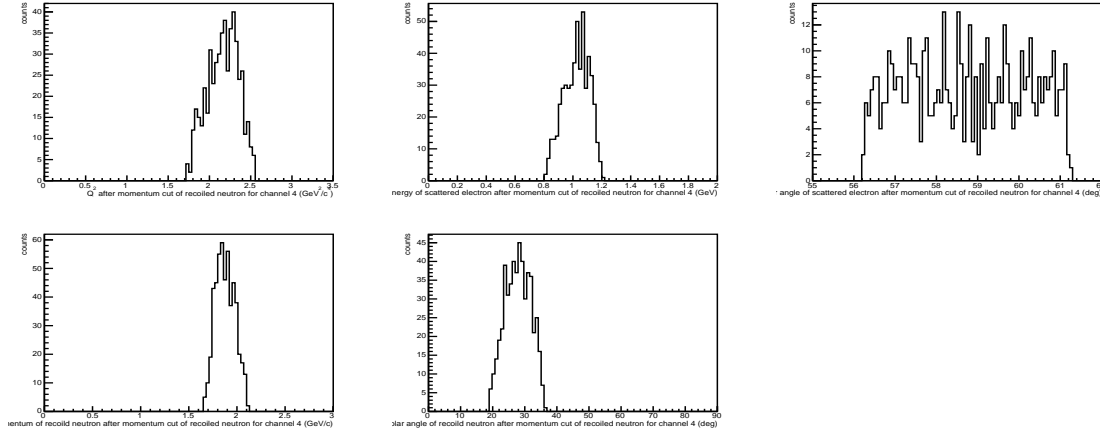


Figure 1.3: Kinematics for channel 4 without filter with momentum of produced proton less than 0.2 GeV/c

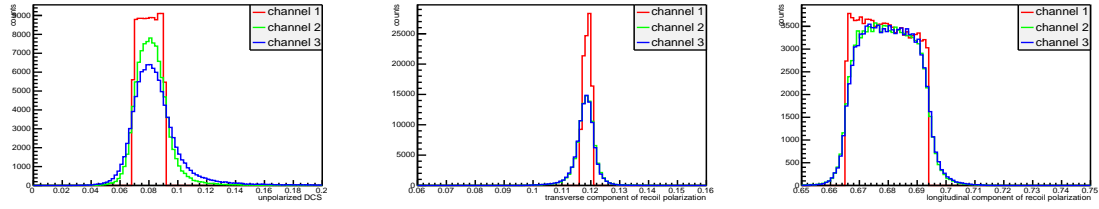


Figure 1.4: DCS information

no filter, the green line denotes unpolarized DCS filter, the blue line denotes polarized DCS filter. After DCS filters are applied, the distributions of Q^2 , E' , θ_e and P_n slightly shift, and the distribution of θ_e becomes more inclined. The kinematic distributions between unpolarized and polarized DCS are very close, which can be explained by the sum of transverse and longitudinal components in Fig.1.6.

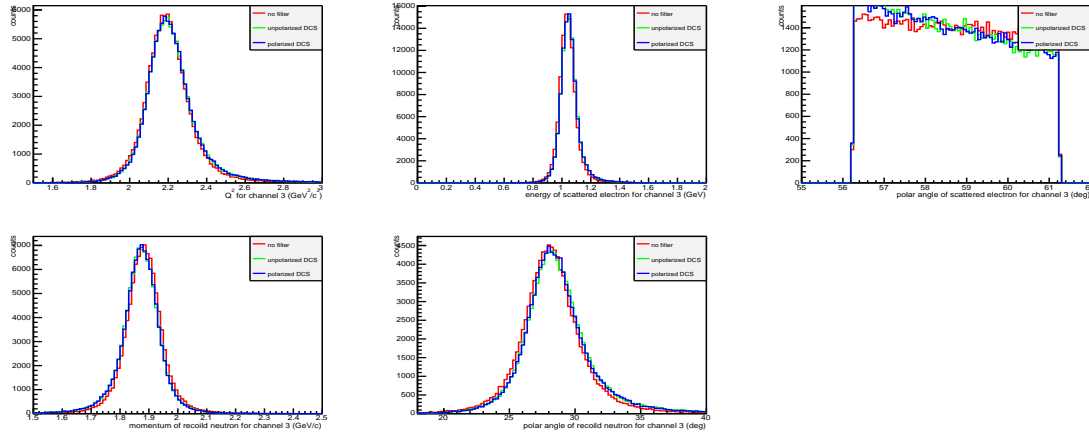


Figure 1.5: Comparisons of Kinematics between filters for channel 3

Figure 1.6 shows transverse, longitudinal components, sum of them, and phase-shift of recoil polarization for channel 3. The variation of the sum is very small, and the distribution is almost flat.

Figure 1.7 shows p_n (top left), E' (top right), Q^2 (bottom left) or θ_e (bottom right) vs θ_n for channel 1 without filter. Red curves represent formulas 1.1 - 1.4 respectively. The phase space calculation by the class JGenPhaseSpace is consistent with the mathematical kinematic solutions.

Figure 1.8 shows p_n (top left), E' (top right), Q^2 (bottom left) or θ_e (bottom right) vs θ_n for

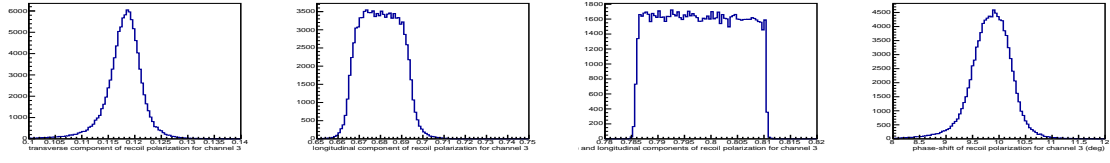
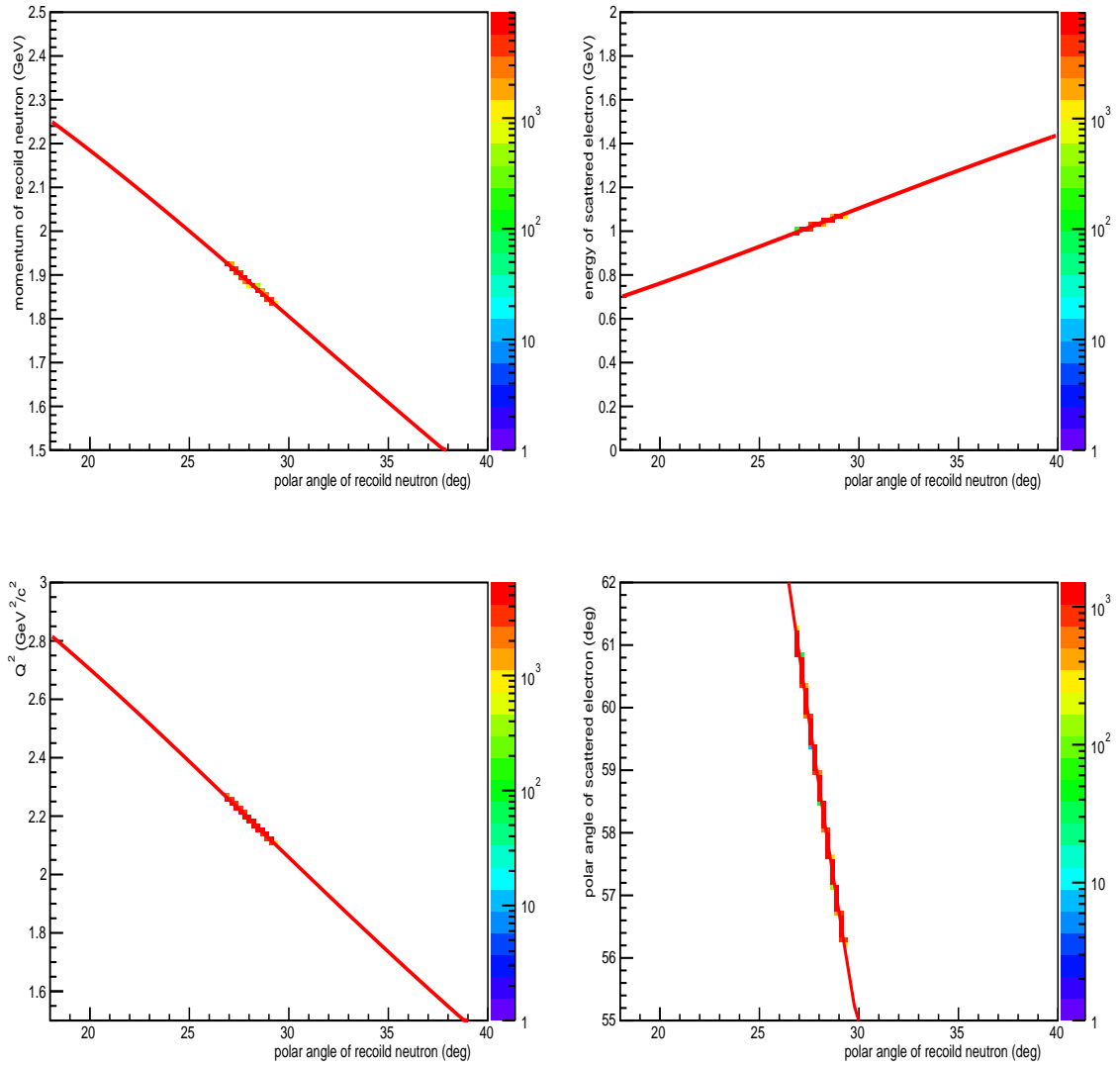


Figure 1.6: Transverse, longitudinal components, sum of them, and phase-shift of recoil polarization for channel 3

Figure 1.7: p_n , E' , Q^2 or θ_e vs θ_n for channel 1 without filter

channel 2 without filter. Red curves represent formulas 1.1 - 1.4 respectively. For the channel 2 where the neutron has Fermi momentum, p_n can be solved by

$$(E + \sqrt{m_n^2 + p_t^2} - \sqrt{m_n^2 + p_n^2})^2 = (E + p_t \cos \theta_t - p_n \cos \theta_n)^2 + (p_t \sin \theta_t \cos \varphi_t - p_n \sin \theta_n \cos \varphi_n)^2 + (p_t \sin \theta_t \sin \varphi_t - p_n \sin \theta_n \sin \varphi_n)^2, \quad (1.14)$$

where p_t , θ_t and φ_t are magnitude, polar angle and azimuthal angle of the neutron target momentum respectively, and p_n , θ_n and φ_n are magnitude, polar angle and azimuthal angle of the recoiled neutron momentum respectively. If $p_t = 0$ (i.e. the target is free), the formula 1.1 is obtained. The term $\sqrt{m_n^2 + p_t^2}$ leads to the deviation of the curve and other terms make the distribution of p_n vs. θ_n fatter than the top left distribution in Fig.1.7 since Fermi momentum is isotropic. E' is expressed as

$$E' = \sqrt{(E + p_t \cos \theta_t - p_n \cos \theta_n)^2 + (p_t \sin \theta_t \cos \varphi_t - p_n \sin \theta_n \cos \varphi_n)^2 + (p_t \sin \theta_t \sin \varphi_t - p_n \sin \theta_n \sin \varphi_n)^2}. \quad (1.15)$$

If $p_t = 0$, this formula becomes the formula 1.2. All terms make the distribution of E' vs. θ_n fatter than the top right distribution in Fig.1.7 and the deviation from the curve is caused by the deviation of p_n . Q^2 is expressed as

$$Q^2 = 2\sqrt{m_n^2 + p_t^2}(E - E') - 2(\vec{p}_e - \vec{p}_{e'}) \cdot \vec{p}_t, \quad (1.16)$$

where \vec{p}_e is momentum of electron beam, $\vec{p}_{e'}$ is momentum of scattered electron, and \vec{p}_t is momentum of the neutron target. This formula is the sum of two terms. Figure 1.9 shows the first term, the second term, and the sum vs θ_n , separately. It figures out the first term leads to the small deviation from the curve, while the second term causes the distribution is very different from the curve. If $p_t = 0$, this formula becomes the formula 1.3. θ_e is expressed as

$$\theta_e = 2 \sin^{-1} \sqrt{Q^2/4EE'} \quad (1.17)$$

where

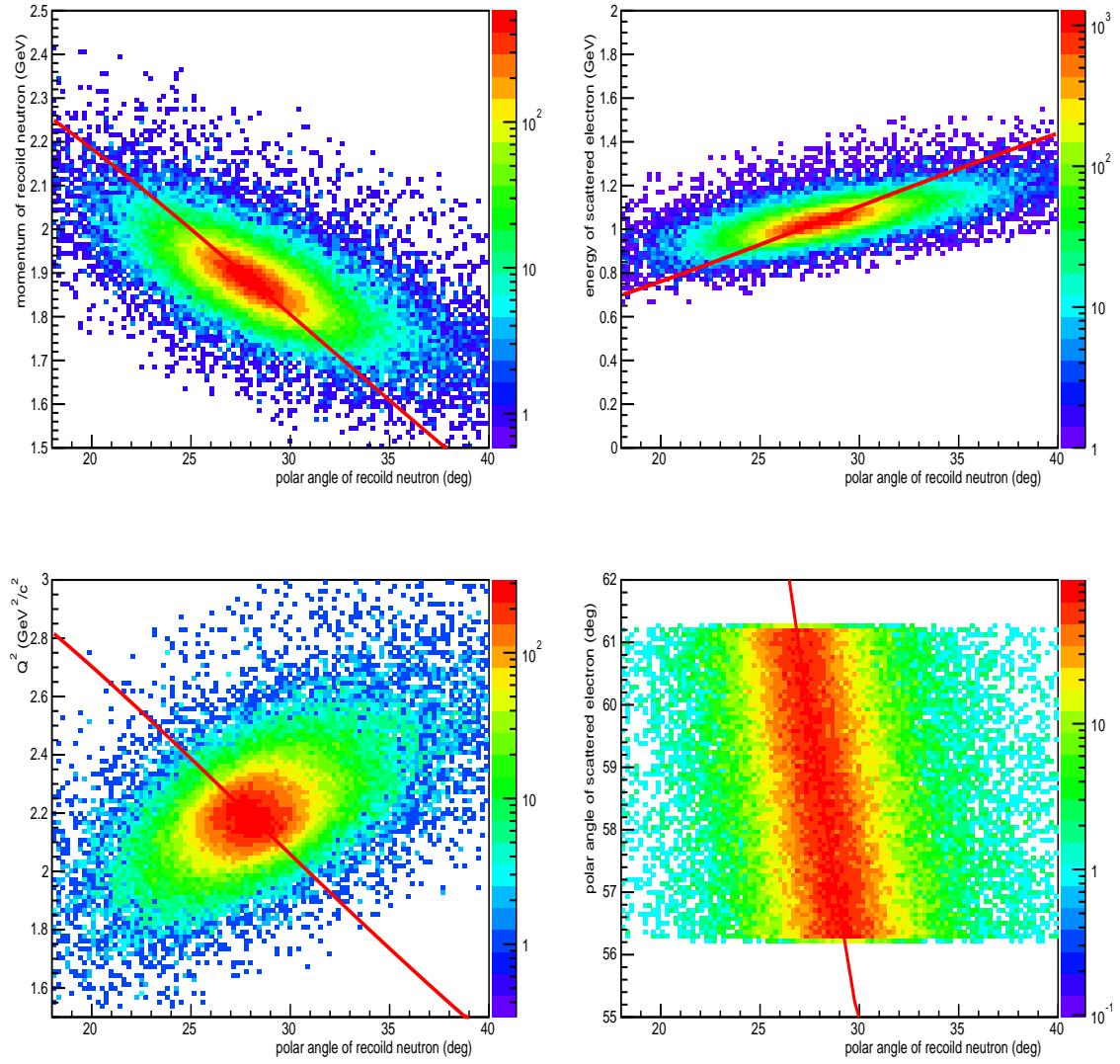
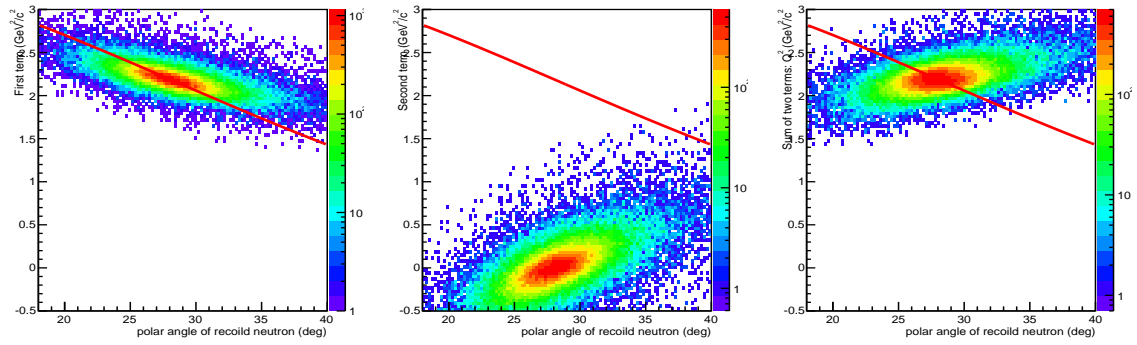
$$Q^2/4EE' = \frac{\sqrt{m_n^2 + p_t^2}(E - E')}{2EE'} - \frac{(\vec{p}_e - \vec{p}_{e'}) \cdot \vec{p}_t}{2EE'} \quad (1.18)$$

is composed of two terms. Figure 1.10 shows the first term, the second term, and the sum vs θ_n , separately. The curves represent $Q^2/4EE'$ as a function of θ_n assuming the target neutron is free. Similarly to Q^2 , the first term leads to the small deviation from the curve, while the second term causes the distribution is very different from the curve. Figure 1.11 shows θ_e vs θ_n when the second term in Eq. 1.18 is canceled or applied. Through the comparison, the effect of the second term on θ_e is checked. If $p_t = 0$, the formula 1.17 becomes the formula 1.4.

Figures 1.12 - 1.14 show p_n (top left), E' (top right), Q^2 (bottom left) or θ_e (bottom right) vs θ_n for channel 3 with no, unpolarized DCS and polarized DCS filters respectively. Red curves represent formulas 1.1 - 1.4 respectively. As consistent with comparisons shown in Fig. 1.5, the distributions here have slight differences between 3 different filters.

Figure 1.15 shows p_n (top left), E' (top right), Q^2 (bottom left) or θ_e (bottom right) vs θ_n for channel 4 without filter. Channel 4 has 3 products, so kinematic distributions are very different from other channels.

Figure 1.16 shows p_n (top left), E' (top right), Q^2 (bottom left) or θ_e (bottom right) vs θ_n for channel 4 without filter with momentum of produced proton less than 0.2 GeV/c. After cut, events are mainly from quasielastic, so the distributions become close to channels 2&3.

Figure 1.8: p_n , E' , Q^2 or θ_e vs θ_n for channel 2 without filterFigure 1.9: The first term, the second term, and the sum of two terms in Eq.1.16 vs θ_n for channel 2 without filter

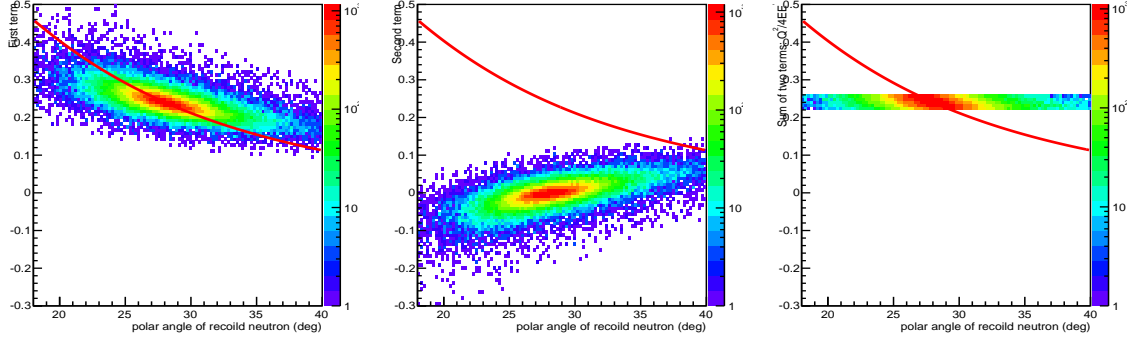


Figure 1.10: The first term, the second term, and the sum of two terms in Eq.1.18 vs θ_n for channel 2 without filter

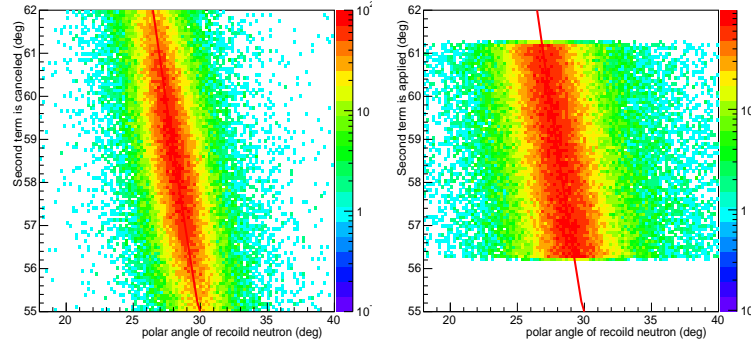
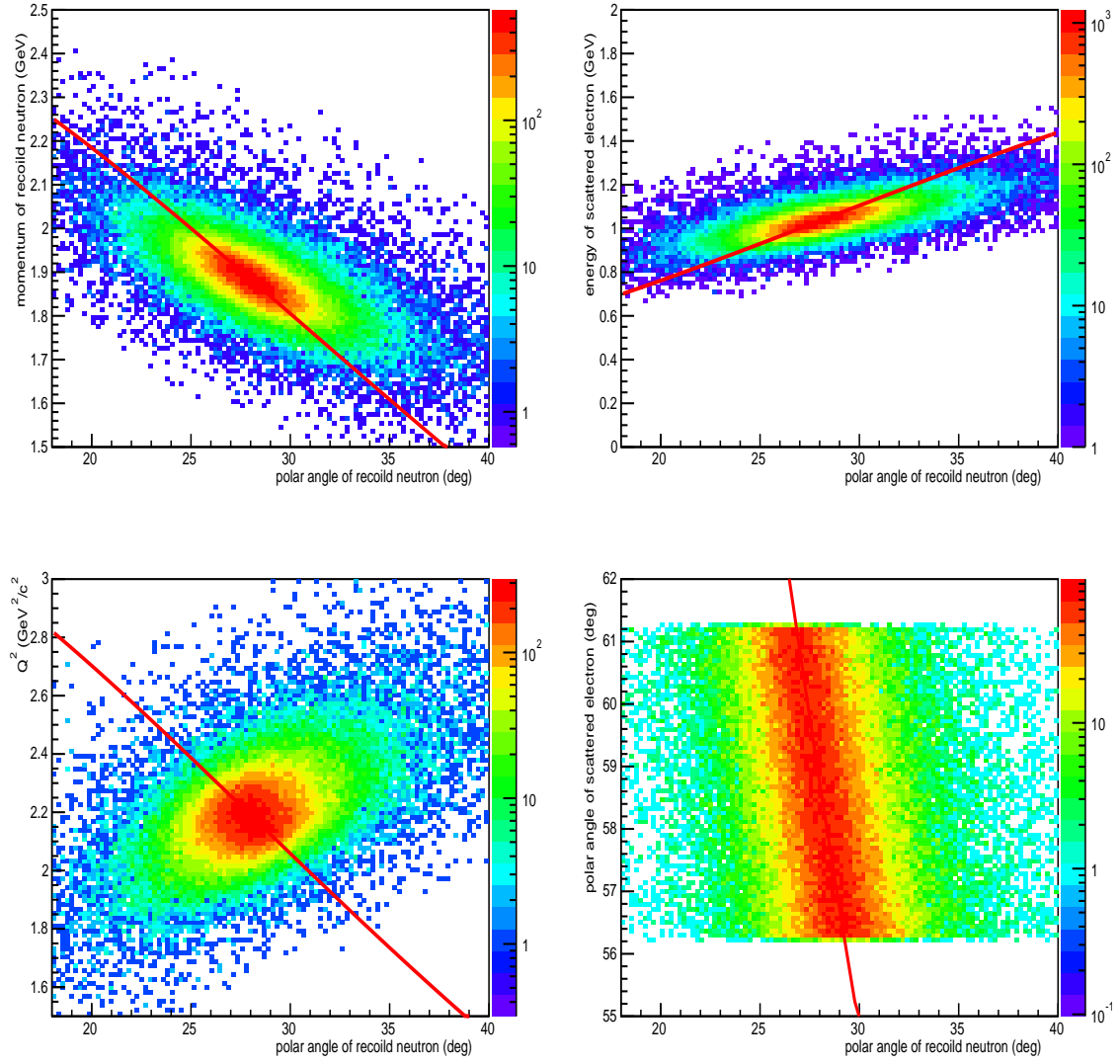


Figure 1.11: θ_e vs θ_n for channel 2 without filter when the second term in Eq. 1.18 is canceled or applied.

1.6 Summary and Future

The first stage of the event generator has been completed. Four parallel channels are built, and there are 3 parallel filters for each channel (channel 4 has no DCS filters currently). 10 files with the electron beam of 2.2 GeV are produced and analyzed.

Next, other electron beam energy setup will be tested. Studies of recoil polarization for $\vec{e}n \rightarrow e\vec{n}$ where target neutron has Fermi momentum, and DCS and recoil polarization for electrodisintegration of deuteron are underway.

Figure 1.12: p_n , E' , Q^2 or θ_e vs θ_n for channel 3 without filter

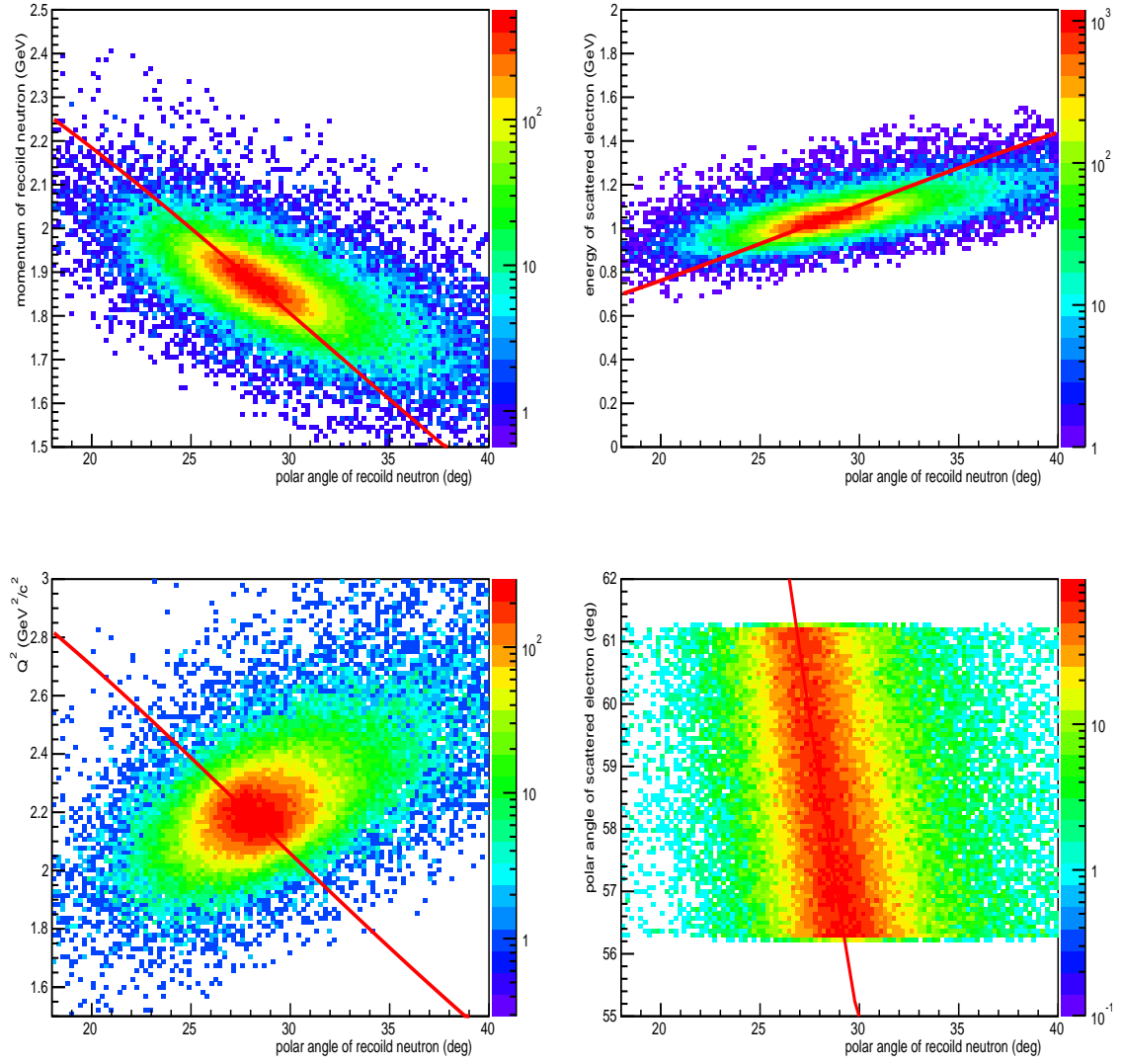
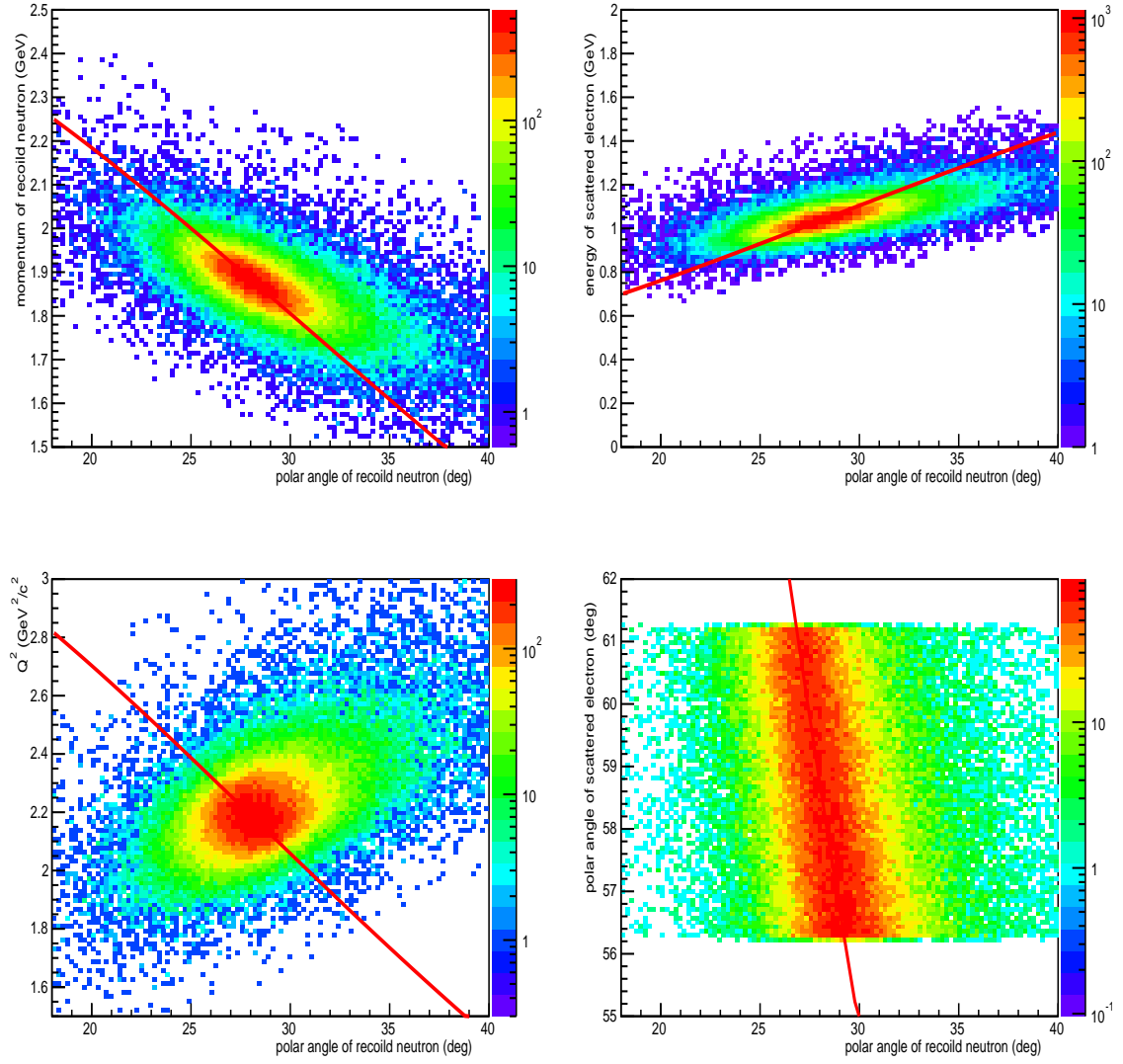
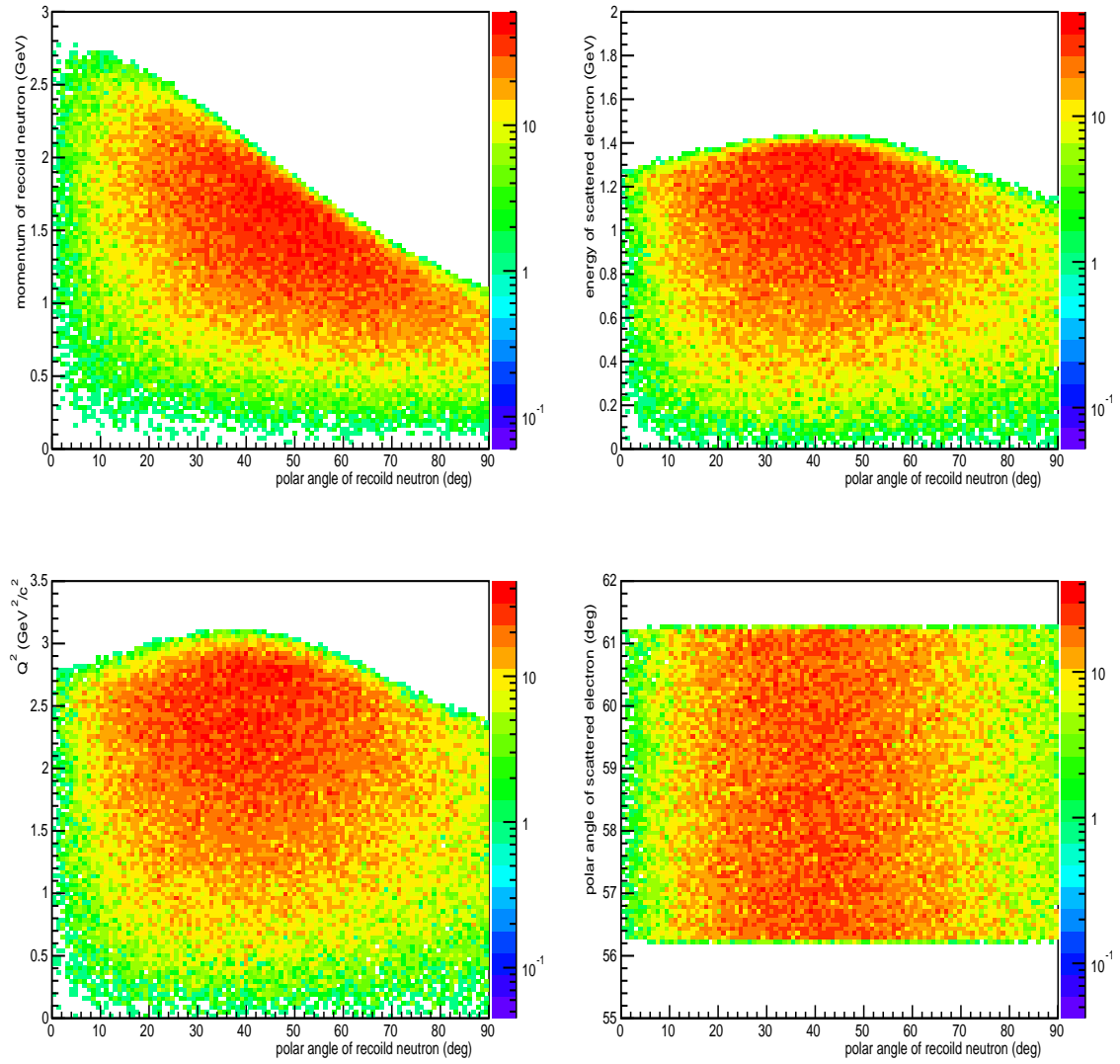


Figure 1.13: p_n , E' , Q^2 or θ_e vs θ_n for channel 3 with unpolarized DCS filter

Figure 1.14: p_n , E' , Q^2 or θ_e vs θ_n for channel 3 with polarized DCS filter

Figure 1.15: p_n , E' , Q^2 or θ_e vs θ_n for channel 4 without filter

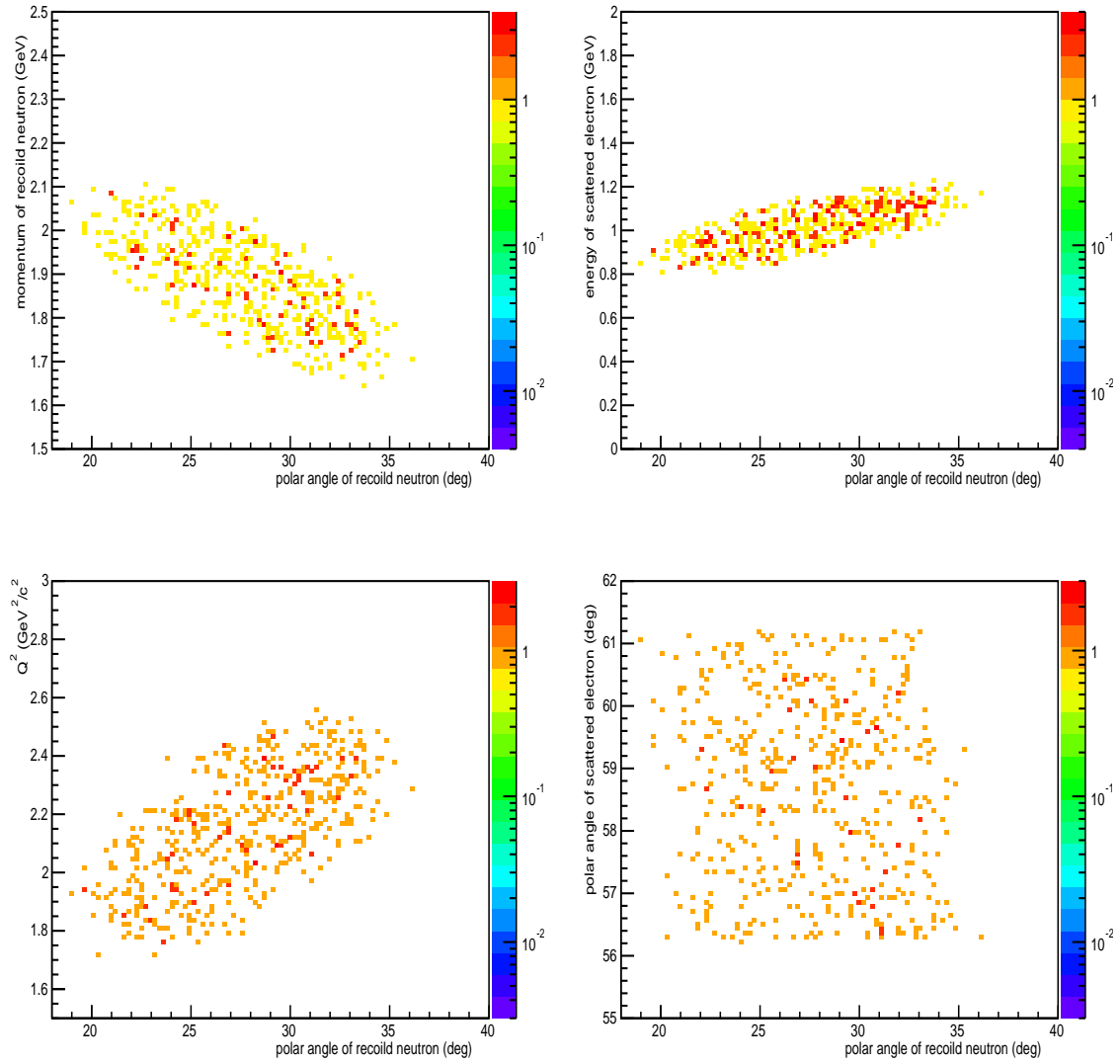


Figure 1.16: p_n , E' , Q^2 or θ_e vs θ_n for channel 4 without filter with momentum of produced proton less than 0.2 GeV/c